

Characterization of non-anechoic chambers and echo cancellation for antenna measurement¹.

Marcos R. Pino, Susana Loredó, Fernando Las-Heras, Tapan K. Sarkar[†]
Department of Electrical Engineering, University of Oviedo.
Campus de Viesques s/n, Edif. 4, 33204 Gijón, Spain. E-mail: flasheras@tsc.uniovi.es
[†]Dept. EE and Computer Science, Syracuse Univ. 121 Link Hall, Syracuse, NY 13244.

Abstract -, This communication focuses on the measurement of antenna radiation patterns when fully anechoic conditions are not available and consequently some undesirable echoes are initially present in the measure. Two techniques are analyzed and compared in order to identify the echo contributions and retrieve the antenna radiation pattern. Their accuracy is evaluated by comparison with measurements obtained in an anechoic chamber.

Introduction

Generally, the measurement of antenna radiation patterns takes place in anechoic chambers, where one attempts to reduce as much as possible the reflected and diffracted contributions from walls and mechanical devices present inside the chamber, using for that appropriate absorbing materials. However, the radiation patterns measured in reverberant or semi-anechoic chambers will certainly present the effects of those undesired contributions, which will yield to inaccuracies in the measured patterns.

In this paper, two techniques are considered and tested to obtain the radiation pattern of antennas from measurements carried out in non-anechoic conditions. For this purpose, a metal plate has been introduced inside an anechoic chamber, which will introduce reflected and diffracted contributions in the measurements. By using the mentioned techniques, these unwanted components will be eliminated from the measurements in order to obtain a radiation pattern as similar as possible to the one obtained in an anechoic chamber. The starting measured data for both techniques will be the chamber frequency response, $S_{21}(f)$, for each of the angles ϕ of the azimuth sweep of the AUT.

Time-gating using FFT

The first technique under consideration estimates the impulse response of the reverberant chamber from its frequency response, by using the inverse Fourier transform. Once in the time domain, it is relatively easy to detect and gate the direct contribution, eliminating the undesired echoes. Applying the Fourier transform to this new time response, where only the direct contribution is present, the radiation pattern can be retrieved at the frequency of interest.

Bearing in mind the relationships that the Fourier transform algorithm establishes between the frequency and the time domains, the bandwidth (BW), the time resolution (Δt) and the step (Δf) of the frequency sweep must be carefully chosen. These parameters will be established as functions of the time delay (δt) from the arrival of the direct contribution until the arrival of the reflected or diffracted contributions

¹ Work supported by the Spanish "MCYT-Ramon y Cajal" program under CAJAL-01-14 and CAJAL-01-15 projects, and by the CICYT-TIC2002-02391 and FICYT-PC-TIC01-08 projects.

(multipath components). This time delay will depend on the separation between the antennas and the location of the obstacles causing the undesired received components. Therefore, the minimum bandwidth required for the frequency sweep can be directly obtained as $BW = 1/\delta t$. However, it is advisable to use a higher time resolution to better distinguish the different contributions in the time domain. On the other hand, the frequency step Δf is chosen as a function of the time response length, taking into account again the distance between the antennas and the location of the main reflecting/diffracting elements located inside the chamber.

Matrix-Pencil Method

The second technique is based on the Matrix-Pencil Method (MPM) [1], an algorithm widely used to approximate functions as sums of complex exponentials. The technique proposed includes the use of the MPM to obtain an approximation of the chamber response (in terms of the $S_{21}(f)$ parameter) as a sum of exponential terms. These complex exponentials can be directly related to the different contributions arriving to the probe (direct, reflected and diffracted components) [2]. The $S_{21}(f)$ response obtained for a given frequency range and azimuth angle ϕ_i will be decomposed as:

$$S_{21}(f_k)_{\phi_i} = \sum_{m=1}^M R_{m,i} e^{s_{m,i} k \Delta f} = \sum_{m=1}^M R_{m,i} z_{m,i}^k \quad \forall k = 0, \dots, N-1 \quad (1)$$

where M is the number of complex exponentials used in the approach and $s_{m,i}$ and $R_{m,i}$ are the coefficients given by the MPM corresponding to the m -th complex exponential term for the i -th angle. The $s_{m,i}$ coefficients provide information about the propagation of each contribution in terms of attenuation and time delay, while $R_{m,i}$ are the amplitudes of each exponential term. The procedure to obtain those coefficients is detailed in [1].

In order to reconstruct the radiation pattern of the AUT, the complex exponential that models the direct contribution propagation for each azimuth angle must be determined. For that purpose, the information about the attenuation and delay of the propagation of the different contributions arriving to the probe provided by the complex coefficients $s_{m,i}$ is used. Considering that the propagation delay of the direct contribution should remain constant for all the azimuth angles, this delay can be easily obtained for the azimuth angle $\phi_0 = 0^\circ$. For this azimuth angle, the direct contribution amplitude ($R_{d,0}$ coefficient) must be greater than the amplitudes of the rest of the exponential terms $R_{l,0}$. Once the direct contribution term is identified for ϕ_0 , the direct contributions for the rest of the azimuth angles are determined comparing their propagation delay with the obtained at ϕ_0 . Then, the radiation pattern of the AUT at the central frequency $f_c = f_k$ (with $k = (N+1)/2$) in full anechoic conditions can be approximated in terms of an amplitude and a complex exponential for each azimuth angle as

$$S_{21}(f_c, \phi_i) = R_{d,i} e^{s_{d,i} c \Delta f} \quad (2)$$

Measurements and Results

The measurements have been carried out in the spherical range measurement system in anechoic chamber located at the University of Oviedo. Both the probe and the AUT were identical pyramidal horn antennas, with an approximately constant gain of 20 dB in the band between 17.7 and 26.7 GHz. They were placed at a height of 2 meters above ground level and separated from each other 5.4 meters. A 2x1 meter rectangular copper plate was placed inside the anechoic chamber, parallel to one of the side walls and to the antennas line of sight, to simulate a partially reverberant chamber.

When the plate is located close to the antennas, the interaction between both (antennas and metal plate) is noticeable in a wide range of azimuth angles as shown in Figure 1, which compares the AUT azimuth pattern measured without and with the metal plate inside the anechoic chamber, at a distance of 1 meter from the antennas. In this situation, the estimated delay for the contribution reflected in the metal plate is 1.2 nsec, therefore in order to achieve an approximate time resolution $\Delta t = \delta t/5$ (to compensate the resolution reduction due to the windowing of frequency data), a bandwidth of 4 GHz was chosen centred at 22 GHz. A frequency step of 5 MHz will provide a time response long enough to avoid aliasing among the most important contributions, giving a total of 801 frequency samples for each azimuth position.

Figure 2 shows the time response of the S_{21} parameter for the different azimuth angles. The presence of the direct contribution can be noticed at all angles, with a propagation time of approximately 18 nsec, and a 1.2 nsec delayed contribution in the $20^\circ - 60^\circ$ azimuth range. Some other less important echoes appear for the lowest azimuth angles, which can be attributed to small reflections produced in the structures supporting the antennas. The elimination of all the contributions with a propagation time greater than 1 nsec guaranties that all the effects due to the metal plate disappear.

Transforming this modified time response back to the frequency domain and plotting the azimuth variation at the frequency of 22 GHz a radiation pattern similar to the one obtained in an anechoic chamber is achieved. Figure 3(a) compares the reference measurement taken under anechoic conditions and the result obtained when the measurement in reverberant conditions is processed in this way.

To apply the Matrix-Pencil technique, the needed frequency bandwidth is estimated as $1/\delta t$. Therefore a total of 151 samples, from $f_0 = 21.6$ GHz to $f_{N-1} = 22.4$ GHz, and an order of $M = 3$ have been set as inputs to the algorithm. In Figure 3(b), a comparison between the reference radiation pattern and the radiation pattern reconstructed with the MPM is plotted.

The accuracy of both techniques has been quantified by the mean value of the error, defined as the absolute value of the difference between the reference and the estimated curve, and the standard deviation of that error. These error values are summarized in Table 1, which also includes the results obtained when the plate distance is 2.05 meters. That is a more favorable situation since the effects of the plate on the radiation pattern are evident in a smaller range of azimuth angles ($30^\circ - 50^\circ$). In the FFT based method, a smaller bandwidth, 1 GHz, is necessary to achieve a time resolution $\Delta t = \delta t/5$ and, consequently, only 201 frequency samples are required for the same Δf . When applying MPM technique, the frequency bandwidth is reduced to 200 MHz (from $f_0 = 21.875$ GHz to $f_{N-1} = 22.125$ GHz) and the number of samples to 51.

Conclusions

Two different techniques have been analyzed to obtain the radiation pattern of antennas from measurements obtained in non-anechoic sites. Both techniques require performing measurements in a frequency range, even though the Matrix-Pencil method requires a smaller bandwidth than the FFT based technique. Another important consideration is that the accuracy of FFT technique is more dependent on the parameters (Δf and BW) that define the frequency sweep. On the other hand, the Matrix Pencil method is quite dependent on the parameter M that defines the number of

exponentials used. The value of M may vary under noisy conditions and may affect to the accuracy of the method.

References

- [1] T. K. Sarkar and O. Pereira, "Using the Matrix Pencil Method to Estimate the Parameters of a Sum of Complex Exponentials", IEEE Antennas and Propagation Magazine, Vol. 37, No. 1, pp. 48-55, February 1995.
- [2] B. Fourestié, Z. Altman, J. Wiart, and A. Azoulay, "On the Use of the Matrix-Pencil Method to Correlate Measurements at Different Test Sites", IEEE Transactions on Antennas and Propagation, Vol. 47, No. 10, pp. 1569-1573, October 1999.

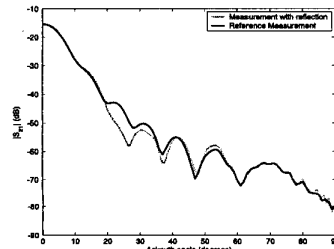


Figure 1. Comparison between the reference measured in an anechoic chamber and the measurement with the metal plate.

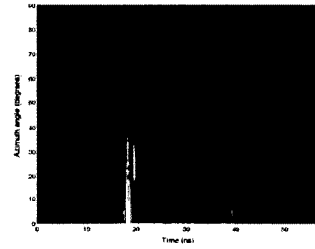


Figure 2. Time response as a function of azimuth angle.

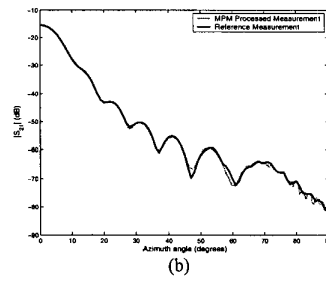
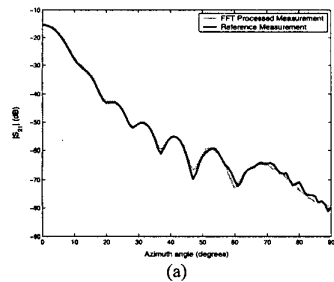


Figure 3. Comparison between the processed results and the reference (metal plate at 1 meter). (a) Using FFT. (b) Using MPM.

Error Measurement	distance: 1m.		distance: 2.05 m.	
	FFT	MPM	FFT	MPM
Mean Error Level (dB)	0.69	0.56	0.60	0.49
Standard Deviation of Error (dB)	0.65	0.67	0.29	0.36
Maximum Error (dB)	3.12	3.03	1.79	1.87

Table 1. Error levels obtained for the processed results using both techniques.